COUNTERACTION OF NON-LINEAR DISTORTION IN A NOVEL MCM-DS-SS WIRELESS LAN RADIO SUBSYSTEM

Paolo Banelli, Saverio Cacopardi, Fabrizio Frescura, Gianluca Reali

Istituto di Elettronica, Università di Perugia -Via G. Duranti 1 - 06125 Perugia - Italy

e-mail: banelli@istel.ing.unipg.it cacopar@istel.ing.unipg.it - frescura@istel.ing.unipg.it - reali@istel.ing.unipg.it

ABSTRACT A novel radio subsystem for WLAN, based on MultiCarrier Modulation DS-SS, is presented. By comparing the obtained performance with the results of the DS-SS physical layer of the standard IEEE 802.11, we point out some important architectural aspects and the factors that may limit performance. In particular, the performance of a base-band pre-distorted non-linear amplifier is analysed by simulations. The analysis of the clipping effect (with and without memory) allows to specify the optimum back-off value in order to balance the bit error rate performance and the efficiency of power amplifiers.

1. *Introduction*

The market trend of mobile computing devices is strongly pushing industry towards the development and the implementation of high speed Wireless Local Area Networks (WLANs). Presently, in this technological area, the only standards delivered by regulatory bodies are the IEEE 802.11 and the ETSI HIPERLAN [1][2]. Since such applications often use bands where electronic devices radiate RF energy (e.g. ISM band), WLANs are primarily affected by interference and multipath fading. In this environment the interference rejection properties of the Spread Spectrum (SS) technique are precious. In fact the SS technique has been adopted in the IEEE 802.11, both in Direct Sequence (DS) and Frequency Hopping (FH) configurations [1]. Moreover, the adoption of the SS technique allows to gain an intrinsic diversity of the signal in order to cope with the effects of multipath fading. In this paper we propose a novel WLAN radio subsystem based on the combination of the SS signalling with the MultiCarrier Modulation (MCM). This combination leads to some interesting technical solutions that exploit the strong issues of both techniques, such as frequency diversity, full channel equalisation by means of a Complex-valued Automatic Gain Control (CAGC) at the receiver side, and rejection of the interference [3]. An MCM-DS-SS radio subsystem for WLAN must be designed taking account of the special issues of such an application. In typical WLAN environment a CSMA/CA (Carrier Sense Multiple Access with Collision Avoidance) access scheme is adopted [1], so the Spread Spectrum technique is only devoted to the rejection of interference and to provide a proper diversity order [4]. Since a good value of throughput has to be guaranteed also for short packets and for MAC messages handshake, great care must be observed in the strategy adopted for the channel estimation and equalisation, by preferring simple to implement techniques, which avoids overhead due to the transmission of dedicated sounding symbols, in order to obtain small values of the processing delay. Moreover, the adoption of MCM makes the consideration of non-linear distortions unavoidable in the design of the system architecture and in performance evaluation. Since Multicarrier Modulations produce non-constant signal envelope, non linear distortions within the transmission chain could endanger system performance significantly. Non linear effects are primarily due to amplifier characteristics and clipping processes [5]. Base-band predistortion could be utilised to counteract such amplifier non linearity. The cascade of a predistortion device and an RF amplifier, globally gives rise to an overall system that can be ideally modelled as an envelope soft-limiting device. The performance analysis of such a device in an MCM-DS-SS system was developed in [6]. In this work however there are some important differences and improvements. First of all, the effects of interpolated clipping are considered with respect to the data clipping analysed in [6]. In addition, the system performance of a feasible predistorting device is analysed. We first present an analytical approach for the linear environment, then we comment the effects of non linear clipping distortion, and finally we present the results obtained by means of simulation trials.

II. *Radio Subsystem Description*

II.1 Modem Scheme

The scheme shown in Fig. 1 is useful to describe the TX and RX base-band sections of the proposed MCM-DS-SS architecture. At the transmitter side the data frame is packed in blocks of μm bits. Each block is then mapped into μ symbols of the M-PSK constellation (with $M=2^m$) according to the Gray code. The resulting complex-valued block is spread by μ periods of a unique spreading sequence. We denote by L the period of the sequence. The spread block is serial to parallel converted in a vector of μL components and then scrambled by a block interleaver of depth equal to μ. The resultant vector feeds an IFFT processor which operates on $L_{fft} > \mu L$ samples. In particular, each vector is padded by $N_1 = \lfloor (L_{fft} - \mu L)/2 \rfloor$ and $N_2 = L_{fft} - N_1$ zeros at its edges. This operation allows it to allocate the transition bandwidth of the transmitter filter.

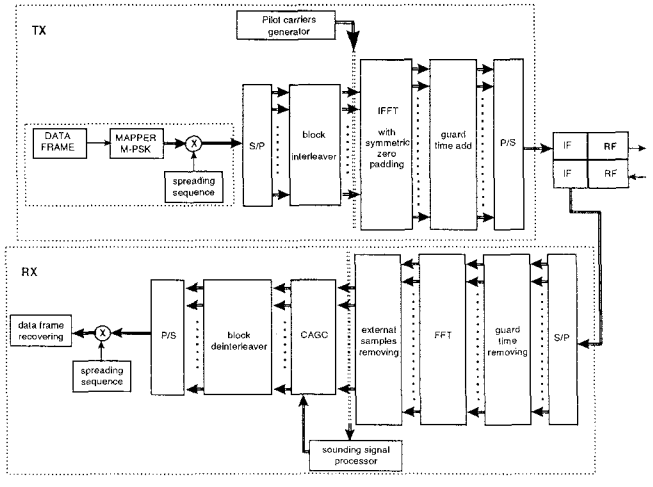

Fig. 1 Basic scheme of the TX and RX base-band sections of the proposed MCM-DS-SS modem. Double lines indicate complex-valued signals.

The sounding signal, which is constituted by a number P_{pil} of known pilot carriers, is interleaved with the data symbols of each MCM symbol, just before the IFFT processing. Since the system operates in a

frequency-selective fading environment, circular prefixes of duration T_g, larger than the delay spread of the channel, are added between adjacent IFFT transformed vectors in order to avoid inter-symbol interference (ISI) and inter-carriers interference (ICI) at the receiver. The resulting vector, after a final parallel to serial conversion, feeds the baseband predistortion and the IF-RF sections. The receiver section of the modems in Fig.1 is dual with respect to the transmitter with the exception of the Complex Automatic Gain Control (CAGC) functional block. From the RF-IF section the received signal is filtered, sampled and serial to parallel converted; then the circular prefix is removed. Since the sounding signal is interleaved in each MCM symbol, the receiver performs an FFT processing on L_{fft} samples, eliminates the zeroes at the edges of the received vector to extract the $\mu L+P_{pil}$ central components, estimates the channel (and consequently the CAGC coefficients) starting from the P_{pil} pilot carriers, and then processes the resulting vector (of μL components) by means of the CAGC and the deinterleaver. After a parallel to serial conversion the signal feeds the spread spectrum receiver and then the data recovering circuits.

II.2 Sounding and Equalisation Techniques

According to the well known *discrete multipath time-domain model*, the received signal can be written as

$$r(t)=\sum_{p=1}^{N_p} h(pT_S,s)S(t-pT_S)+n(t), \tag{1}$$

where $h(pT_s,s)$ $p=1,2,..,N_p$ is the sampled, space-variant, complex-valued impulse response of the channel, i.e. $h(pT_s,s)$ is the complex-valued coefficient that corresponds to the pth path. T_S is the time duration of the transmitted samples, $S(t)$ is the transmitted signal, N_p is the number of paths of the channel, $n(t)$ is the Additive White Gaussian Noise (AWGN). The maximum value N_pT_S of the time delay represents the channel *delay spread*. Because of the small random variations of the environment and, if it is the case, the user mobility, the space-variant nature of the channel translates itself in a time dependence of the channel impulse response. If the duration $T_b=L_{fft}T_S$ of the OFDM symbols (L_{fft} components) is considerably smaller than the coherence time ($\Delta T_c=1/f_D$, f_D being the maximum Doppler frequency) of the channel, the slow fading channel condition is maintained, thus expression (1) can be written as

$$\mathbf{R}=\mathbf{h}*\mathbf{S}+\mathbf{N} \tag{2}$$

In (2) the symbol "*" denotes the linear discrete convolution, $\mathbf{S}=[s_1,s_2,....,s_{L_{fft}}]$ and $\mathbf{R}=[r_1,r_2,...,r_{L_{fft}+N_p-1}]$ are the transmitted and received vectors respectively, $\mathbf{N}=[n_1,n_2,...,n_{L_{fft}+N_p-1}]$ is the AWGN vector and $\mathbf{h}=[h_1,h_2,...h_{N_p}]=[h(T_S,s),h(2T_S,s)...h(N_pT_S,s)]$ is the discrete channel impulse response at the sounding time. It is evident that, because of noise, the more powerful the transmitted sounding signal is, the more accurate the channel estimation is. For this purpose we denote as S/D the energy ratio between the sounding and the data symbols. In [6] a sounding block was transmitted at the beginning of a data packet and every a certain number of MCM blocks. In this case, vice versa, the sounding signal is interleaved with data, in each MCM symbol, before the IFFT processing at the transmitter, according to a technique similar to the one adopted in the Digital Video Broadcasting (DVB-T) standard [7]. The sounding vector is defined as

$$S_{pil}[k]=\sqrt{\frac{\gamma_p}{P_{pil}}}\sum_{n=0}^{P_{pil}-1}F_{SC}[k]\delta(k-n(L+1)),\ 0\le k\le \mu L+P_{pil}, \tag{3}$$

where P_{pil} is the number of pilot carriers in each MCM block, γ_p is the energy value of the sounding vector and $\mathbf{F}_{SC}$, with $|F_{SC}[k]|=1$, is a random complex valued vector which is adopted to scatter the pilot carriers in order to reduce the crest-factor (the ratio between the peak and the mean power) of the transmitted signal.

In the proposed system configuration F_{SC} is a FZC sequence [8], expressed as

$$\mathbf{F}_{SC}[k]=\begin{cases} e^{j\frac{Q\pi}{P_{pil}}k^2} & ,P_{pil}\ \text{even} \\ e^{j\frac{Q\pi}{P_{pil}}k(k+1)} & ,P_{pil}\ \text{odd} \end{cases} \tag{4}$$

Q being an integer relatively prime to P_{pil}. Equation (4) defines a polyphase sequence with a periodic autocorrelation function that is not zero only in the trivial case of sequence alignment. As a consequence, such sequences exhibit flat power spectra in the discrete time domain [9]. The choice of the FZC sequences for the pilot carriers gives rise to a sounding MCM signal (i.e. signal without data carriers) characterised by a crest-factor of about 2.6/2.7 dB (depending on the P_{pil} value). This value is comparable with the minimum values obtainable by the Newman's sequences [10]. The adopted sounding signal, combined (i.e. summed) with the data signal, produces an overall signal with reduced crest-factor with respect to other phase choices for the pilot carriers. Starting from the data vector $\mathbf{d}=[d_1,d_2,...,d_{\mu L}]$, the vector

$$\mathbf{D}_{pil}=[0,d_1,d_2,..,d_L,0,d_{L+1},d_{L+2},..,d_{2L},0,..,d_{(\mu-1)L+1},d_{(\mu-1)L+2},..,d_{\mu L},0], \tag{5}$$

is obtained by interleaving P_{pil} zeroes in the positions corresponding to the pilot carriers in (3). After the combination of sounding and data signals

$$\mathbf{S}=\mathbf{S}_{pil}+\mathbf{D}_{pil} \tag{6}$$

the resulting vector $\mathbf{S}$ is IFFT processed and transmitted. At the receiver side, after the FFT processing on L_{fft} samples and the elimination of the virtual carriers to extract the $\mu L+P_{pil}$ central components, the estimation of the channel is obtained first by extracting the P_{pil} pilot carriers (in the following the symbol "$\otimes$" and "$\div$" denote a complex multiplication and a division, component by component, respectively)

$$\hat{\mathbf{D}}_{pil}=\mathbf{R}_{fft}\otimes\mathbf{M}\div\mathbf{F}_{SC},\ \mathbf{M}=[\overbrace{1,\underbrace{0,0,..0}_{L},1,\underbrace{0,0,..0}_{L},1,..,\underbrace{0,0,..,0}_{L},1}^{\mu L+P_{pil}}], \tag{7}$$

$\mathbf{R}_{fft}$ being the received vector (2) after the FFT processing, then by interpolating the resulting vector (7) to provide $\hat{\mathbf{H}}=[\hat{h}_{N_1+1},\hat{h}_{N_1+2},...\hat{h}_{L_{fft}-N_2}]$, which represents the estimation of the channel transfer function. An improvement of the quality of the estimation of the channel is obtained by filtering the $\hat{\mathbf{H}}$ by means of a *zero-phase forward and reverse digital filter*, whose pass-band is determined according to the frequency spacing of the pilot carriers and to the coherence bandwidth of the channel.

The CACG coefficients are obtained from the estimated channel response $\hat{\mathbf{H}}$, as the conjugate of each component, according to the *Maximum Ratio Combining* equalisation technique [6][12]:

$$C[k]=\tilde{H}^*[k],\quad k=N_1+1,...,L_{fft}-N_2. \tag{8}$$

II.3 Model of ideal pre-distorted power amplifiers

A non-linear power amplifier can be modelled as a memoryless device

when the signal bandwidth is narrow with respect to its passband [13]. If the signal at the input of a non linear amplifier is expressed by its complex base-band representation

$$s(t) = R(t) \cdot e^{j\vartheta(t)} \tag{9}$$

the non linear distorted output is

$$s_d(t) = H[R(t)] \cdot e^{j[\vartheta(t)+\Phi[R(t)]]} \tag{10}$$

where $H[R]$ and $\Phi[R]$ are known as AM/AM and AM/PM distortion curves respectively. The base-band pre-distortion is a well known technique for the compensation of the non linear distortion introduced by an RF power amplifier. By use of this technique the magnitude $R(t)$ of the input signal is predistorted by two curves $G[R]$ and $\Psi[R]$ that globally invert $H[R]$ and $\Phi[R]$ [11]. In this paper we consider a non linear amplifier whose distortion curves are shown in Fig. 2. The predistortion strategy belongs to the category of signal predistortion, since the predistorter operates not on data at the output of the OFDM modulator, but on the digital interpolated baseband signal before the A/D conversion, as shown in Fig. 3. The predistorter, whose a possible architecture is shown in Fig. 3, is based on memory storing of the predistorting curves $G[R]$ and $\Psi[R]$ [13][14].

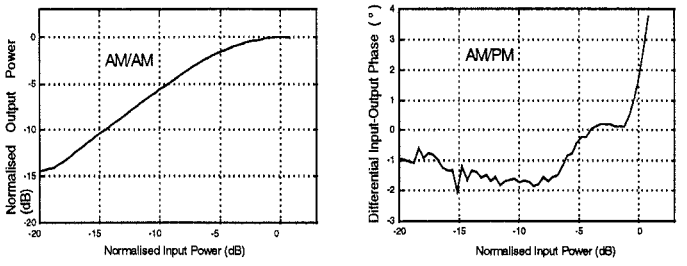

Fig. 2 AM/AM and AM/PM distortion curves of the considered RF power amplifier

The interpolation order required to obtain a good compensation depends on the class of the amplifier [14]. Since we considered a class AB Solide State Amplifier (see AM/AM and AM/PM curves), an interpolation factor of 4 is enough to guarantee a good predistortion. A signal quantization of 10 bits is also adopted in the simulations. An ideal predistorter that perfectly inverts the non linear characteristics of the power amplifier produces a global system without AM/PM distortion and with a residual AM/AM one, that, because of the maximum output power of the RF Amplifier, may be modelled as a soft limiting device.The residual soft limiting AM/AM produces a distortion of the transmitted signal due to the high peak to mean value ratio that characterises OFDM signals.

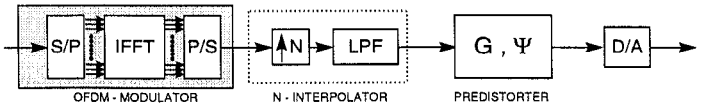

Fig. 3a

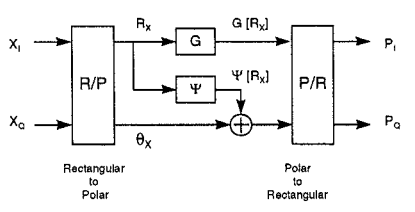

Fig. 3b

Fig. 3 A feasible configuration for the base-band predistortion subsystem (Fig. 3a). A zoom view of the predistorter block (Fig. 3b).

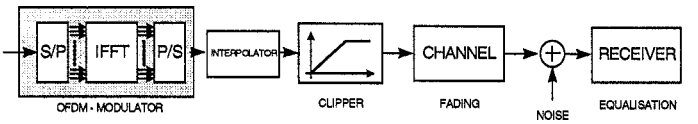

Fig. 4 A model for a MCM system with an ideally predistorted power amplifier

Therefore, the system performance for an ideal predistorted amplifier can be investigated by using the system model shown in Fig. 4.

II.4 Effects of Magnitude Clipping of an OFDM signal

The complex base-band representation of the OFDM data samples transmitted during each period T_b is:

$$\hat{s}[n] = \hat{s}(nT_s) = IFFT\{\hat{z}_k\} = \sum_{k=0}^{L_{fft}-1} \hat{z}_k e^{j\frac{2\pi}{L_{fft}}kn}, \quad n = 0,\ldots,L_{fft}-1 \tag{11}$$

where $\hat{z}_k = a_k + jb_k$ represents the unmodulated complex information symbols.

If the number L_{fft} of carriers is sufficiently high, and the real symbols a_k, b_k are modelled statistically so that

$$\begin{aligned} &E\{a_i b_j\} = 0 \quad \forall i,j \\ &E\{a_i a_j\} = E\{b_i b_j\} = 0, \quad i \neq j \\ &E\{a_k^2\} = E\{b_k^2\} = \sigma_0^2 \quad \forall k, \end{aligned} \tag{12}$$

$E\{\cdot\}$being the expected value, then, because of Central Limit Theorem, $\mathrm{Re}\{s[n]\}$ and $\mathrm{Im}\{s[n]\}$ are distributed as gaussian random variables and, therefore, the signal magnitude $R[n] = \sqrt{\mathrm{Re}\{s[n]\}^2 + \mathrm{Im}\{s[n]\}^2}$ is Rayleigh distributed. Under the above hypothesis the distortion effects of magnitude clipping can be analysed as proposed in [6] or alternatively by use of Bussgang's theorem [15]. The theorem states that the output of a non linear device driven by a gaussian input can be expressed as the sum of two uncorrelated signals. The former, which represents the useful part, is just an attenuated replica of the input, and the latter represents a distortion signal uncorrelated with the input. So, if $\hat{s}_c$ is the clipped signal, we can express it by

$$\hat{s}_c = \hat{s}_u + \hat{d}_c = g \cdot \hat{s} + \hat{d}_c \tag{13}$$

g being the attenuation factor of the useful signal, and d_c the distortion signal. It can be shown that the useful output power may be expressed as

$$P_u = E\left\{\left|\hat{S}_u\right|^2\right\} = g^2(IBO) \cdot E\left\{\left|\hat{S}\right|^2\right\}$$

$$g(IBO) = \frac{1}{2}\sqrt{\pi \cdot IBO} \cdot erfc\left(\sqrt{IBO}\right) + 1 - e^{-IBO} \tag{14}$$

$E\left\{\left|\hat{S}\right|^2\right\}$ is the clipper input power, $c = A_c/\alpha$ is the so called *'clipping ratio'*, $IBO = c^2/2$ is the Input Back-Off (IBO) of the pre-distorted power amplifier and $erfc(x)$ is the complementary error function, that is $erfc(x) \equiv 1 - \frac{2}{\sqrt{\pi}}\int_0^x e^{-t^2}dt$. The total output power is expressed by [6]

$$P_c = E\left\{\left|\hat{S}_c\right|^2\right\} = \Gamma(IBO) \cdot E\left\{\left|\hat{S}\right|^2\right\} \tag{15}$$

$\Gamma(IBO) = 1 - e^{-IBO}$ being the input-output attenuation power. Because of the uncorrelation stated by Bussghang's theorem, the clipping distortion power is simply expressed by:

$$P_d = E\left\{\left|\hat{d}_c^2\right|\right\} = P_c - P_u = E\left\{\left|\hat{s}^2\right|\right\} \cdot \left[\Gamma(IBO) - \gamma^2(IBO)\right] \qquad (16)$$

In the proposed sounding technique, the data carrier signal $\mathbf{D}_{pil}$ of (5) follows the hypothesis of complex gaussian distribution stated by (12). If the $\mathbf{S}_{pil}$ sounding component is gaussian distributed, the overall MCM signal $\mathbf{S}$ of (6) is a complex-valued gaussian signal too. This assumption requires a random phase modulation of each pilot carrier. On the contrary, we have chosen to establish a fixed analytical relation between each carrier phase, as stated in (4), in order to obtain both a low peak-to-mean value of the sounding signal and a considerable reduction of the crest factor of the overall signal. This effect can be outlined by the histograms that characterise the signal probability distribution, as shown in Fig. (5) for an S/D value of -3.0 dB.

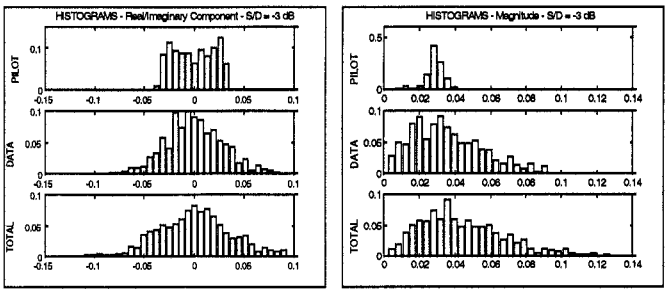

Fig. (5) Histograms of the real/imaginary parts and the magnitude of the Pilot signal, the data signal and their combination according to expressions (5) and (6).

The total signal is characterised by a mean power that is the sum of the two frequency orthogonal signal powers. It exhibits a distribution with peak values that are not much greater than the data signal. As a consequence, the crest factor is reduced. This reduction implies a smaller sensitivity of the MCM signal to the clipping phenomenon and, consequently, a lower practical IBO for the predistorted amplifier. However, this power gain in terms of reduced IBO is paid as a lower power efficiency. Indeed, only a part of the total signal power is dedicated to the data transmission depending on the sounding-to-data power ratio S/D. Further considerations about this particular aspect will be provided in the numerical results.

II.4 Frame Description

Table 1 shows the most significant system parameters of the proposed configuration. In order to make a number of considerations and comparisons possible, in the following we will assume as a reference some of the system and frame parameters of the IEEE 802.11 Draft Standard [1].

MCM-DS-SS WLAN SYSTEMS PARAMETERS			
MAX DELAY SPREAD (s)	1.00E-06	CARRIER FREQUENCY (Hz)	2.40E+09
COHERENCE BANDWIDTH (Hz)	1.00E+06	MAX SPEED RX-TX (m/s)	1.00
CHANNEL BANDWIDTH (Hz)	1.10E+07	MAX DOPPLER SPREAD (Hz)	8.00
CHIP RATE (chip/s)	1.10E+07	CHANNEL COHERENCE TIME (s)	1.25E-01
CHIP DURATION (s)	9.09E-08		
CIRCULAR PREFIX LENGTH (chips)	11		
FRAME MAX LENGTH (bytes)	2400	VIRTUAL CARRIERS	31
FFT LENGTH (samples)	512	MCM CARRIERS SPACING (Hz)	21484.375
SPREADING FACTOR	11	PILOT CARRIERS SPACING (Hz)	252048.399
DATA SYMBOLS / MCM SYMBOL	40	GUARD BAND (kHz)	666.02
DATA SYMBOLS MAPPING	8-PSK	MCM SYMBOL RATE (symbol/s)	21032
BITS / MCM SYMBOL	120	DATA BLOCK RATE (blocks/s)	21032
BYTES / MCM SYMBOL	15	MCM SYMBOL DURATION (s)	4.7547E-05
EFFECTIVE BITS / MCM SYMBOL	120	SOUNDING PERIOD (s)	4.7547E-05
MCM DATA SYMBOLS / FRAME	160	BIT RATE (bit/sec)	2523840
DATA CARRIERS	440	SYMBOL RATE	841280
PILOT CARRIERS	41		

Table 1 System parameters of the proposed OM-DS-SS WLAN system.

By looking at Table 1, we can make the following considerations:
The proposed system configuration is characterized by the same chip rate and the same spreading factor L of the IEEE 802.11 DS-SS Physical Layer Specifications [1].

- The measured maximum channel delay spread is 1 μs, that leads to a coherence bandwidth of 1 MHz. By comparing these values with the spreading factor L and the channel bandwidth it is possible to conclude that the proposed system achieves a full exploitation of the diversity order of the channel.
- The FFT length is 512. This value represents a good trade-off among some aspects such as: efficiency with respect to the adoption of a circular prefix between adjacent MCM blocks, system throughput for short packets and for MAC messages handshake, implementation of a real-time FFT / IFFT processor.
- The comparison of the pilot carriers spacing with the channel coherence bandwidth leads to the expectation of a good behaviour of the system in the estimation of the channel response.
- The maximum achievable bit rate is 2.523.840 bit/s. Taking into account the value of the channel bandwidth of 11 MHz it can be concluded that the proposed system configuration show a maximum spectral efficiency value more than doubled with respect to the IEEE 802.11 (2 Mbit/s in one channel of 22 MHz).

Fig. 6 shows the frame structure of the proposed MCM-DS-SS radio access scheme. A frame of 2400 bytes is segmented into 160 MCM symbols. The sounding signal is embedded in each MCM block containing 40, 8-PSK symbols corresponding to 15 bytes. Since no dedicated sounding block is required, the shortest allowed block is represented by a single 15 bytes data block.

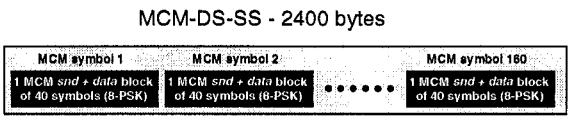

Fig. 6 Frame format of the OM-DS-SS radio access schemes.

III. Performance Analysis in Linear Environment

Equation (2) represents the signal expression, in the time domain, at the receiver side. For sake of notation simplicity in the following we avoid the mathematical details related to the sounding of the channel. When transmission of data is considered, the signal vector S is obtained as

$$\mathbf{S} = IFFT\{\mathbf{D}\}, \quad \mathbf{D} = [\underbrace{0,0,..,0}_{N_1}, d_1, d_2, \ldots, d_\mu, \overbrace{\underbrace{0,0,\ldots,0}_{N_2}}^{L_{fft}}], \qquad (17)$$

$\mathbf{D}$ being the spread, interleaved and zero-padded data vector. Provided that the guard time T_g is correctly sized in order to avoid ICI and ISI interference, after the FFT processor each received vector may be written as

$$\mathbf{R}_{fft} = [R_1, R_2, \ldots, R_{L_{fft}}] = FFT\{\mathbf{R}\} = \mathbf{H} \otimes \mathbf{D} + \mathbf{N}_{fft} \qquad (18)$$

In (18) $\mathbf{H} = [H_1, H_2, \ldots H_{L_{fft}}]$ is the channel frequency response and $\mathbf{N}_{fft} = [N_1, N_2, \ldots, N_{L_{fft}}]$ is the FFT transformed AWGN vector.

Equation (18) means that each component of the data vector $\mathbf{D}$ is multiplied by a complex-valued coefficient, viz. a sample of the instantaneous transfer function of the channel.
After the CAGC processing, the received signal is written as:

$$\mathbf{Y} = \mathbf{C} \otimes \mathbf{R}_{fft} = \mathbf{C} \otimes \mathbf{H} \otimes \mathbf{D} + \mathbf{C} \otimes \mathbf{N}_{fft}, \mathbf{C} = [\underbrace{0,0,..,0}_{N_1}, \overbrace{c_1, c_2, .., c_{\mu L}}^{\mu L}, \underbrace{0,0,..0}_{N_2}], \qquad (19)$$

where the $c_1, c_2, \ldots, c_{\mu L}$ are calculated according to (8). After deinterleaving and despreading of the $\mathbf{Y}' = \mathbf{Y}[N_1+1, \ldots, L_{fft} - N_2]$ vector, formed by the μL non-zero components of the vector (19), the detected M-PSK symbols are obtained. In particular, each M-PSK symbol is obtained by a threshold decision of the scalar product of the spreading code and the relative segment of the $\mathbf{Y}'$ vector as follows:

$$p^{(j)} = trsh\left(\mathbf{b} \bullet \mathbf{y}'_{(j)}\right), \quad \mathbf{y}'_{(j)} = [y'_1, y'_2, \ldots, y'_L] = \mathbf{Y}'[(j-1)L+1, \ldots, jL], \quad (20)$$

where $p^{(j)}$ is the jth decoded M-PSK symbol, *trsh(.)* is the threshold decision function, and $\mathbf{b} = [b_1, b_2, \ldots, b_l, \ldots, b_L]$, $b_l \in \left\{-1/\sqrt{L}, +1/\sqrt{L}\right\}$ is the spreading sequence. The symbol " $\bullet$ " denotes the scalar product. To obtain an expression for the BER, we now consider the detection of the generic M-PSK symbol $p^{(j)}$. The scalar product in (20) can be expanded as

$$\mathbf{b} \bullet \mathbf{y}'_{(j)} = \sum_{l=1}^{L} b_l c_l \left(h_l b_l p^{(j)} + n_l\right) = \underbrace{\frac{p^{(j)}}{L} \sum_{l=1}^{L} c_l h_l}_{a} + \underbrace{\sum_{l=1}^{L} b_l c_l n_l}_{b}. \quad (21)$$

In (21) the first summation of the right hand side represents the useful signal, while the second summation is due to noise. To take into account the effect of the channel sounding on the performance, the CAGC coefficients c_l can be rewritten as

$$c_l = c'_l + n_l', \quad c'_l = h_l^*. \quad (22)$$

Each coefficient in (22) is modelled as the sum of two contributions. The former is obtained by an ideal sounding operation, the latter is a noise term that takes into account the real sounding. By means of (22), expression (21) may be rewritten as

$$\mathbf{b} \bullet \mathbf{y}'_{(j)} = \underbrace{\frac{p^{(j)}}{L} \sum_{l=1}^{L} c'_l h_l}_{a} + \underbrace{\frac{p^{(j)}}{L} \sum_{l=1}^{L} n'_l h_l}_{a'} + \underbrace{\sum_{l=1}^{L} b_l c'_l n_l}_{b} + \underbrace{\sum_{l=1}^{L} b_l n'_l n_l}_{b'}. \quad (23)$$

The interleaver makes the h_l coefficients, and consequently the c'_l coefficients, independent of the l index, thus if we now consider the energy values related to the various contributions in (23), we obtain:

$$\begin{aligned} &(a).\ E_a \cong E_p \, \mathrm{E}\left\{\left|c'_l h_l\right|^2\right\}, \quad (a').\ E_{a'} \cong E_p \sigma_n^2 \, \mathrm{E}\left\{\left|h_l\right|^2\right\} \\ &(b).\ E_b \cong \sigma_n^2 \, \mathrm{E}\left\{\left|c_l\right|^2\right\}, \quad (b').\ E_{b'} \cong \sigma_n^2 \sigma_n^2 \end{aligned} \quad (24)$$

In (24) E_p is the mean energy value of the M-PSK symbols, $\mathrm{E}\{.\}$ is the expected value, σ_n^2 and $\sigma_{n'}^2$ are the variances of the noise related to the data and to the sounding, respectively. In particular, the value of the variance $\sigma_{n'}^2$ depends on the sounding technique adopted and on the energy of the sounding signal. The noise contributions, (a'),(b) and (b') in (21) are independent and Gaussian. Their sum is a zero-mean Gaussian distribution with a variance equal to the sum of the respective variances, so, taking into account the threshold decision (20), the BER for the M-PSK scheme is upper bounded by:

$$BER\big|_{M-\mathrm{PSK}} \le \frac{1}{\log_2(M)} erfc\left\{\sin\frac{\pi}{M}\sqrt{\frac{E_a}{\left(E_{a'} + E_b + E_{b'}\right)}}\right\}. \quad (25)$$

Expression (25) represents an upper bound for the BER under the hypothesis of time-invariant channel, i.e. the estimation error on the values of the CAGC coefficients is due only to the noise related to the sounding operation. The time-variant nature of the channel produces a performance penalty which depends on the speed of the mobile user. Nevertheless, in WLAN applications, the user is typically fixed or its speed is low enough to make (25) a good approximation of the actual performance.

IV. Numerical Results

A first set of simulation trials has been carried out in order to point out the following aspects:

Crest Factor: this key parameter has a great impact on the implementation issues of MCM systems, since it gives a measure of the dynamic range required by the power amplifier of the TX section of the modem.

BER performance in linear environment: starting from a set of measured channel delay profiles, the statistical parameters (24) are calculated numerically. The values are substituted in (25) in order to obtain the BER performance for different values of the S/D ratio. Simulation trials, using measured delay profiles in NLOS conditions, have been carried out to validate the results.

Figure 7 shows the crest factor of the proposed system configuration for different values of the S/D ratio. The values shown in figure 7 are the mean values of the crest factor observed in each MCM symbols. The *data crest factor* refers to the IFFT data output before interpolation, while the *signal crest factor* refers to the signal after the interpolation process shown in Figure 3, so the corresponding values are very significant since they represent the real dynamic range of the transmitted signal.

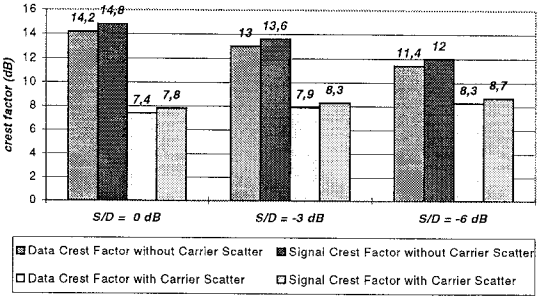

Fig. 7 Crest factor of the MCM-DS-SS architecture for different values of the S/D ratio.

It is evident how the carrier scattering produces a significant reduction of the crest factor values. The crest factor values, without the carrier scattering, decrease, as expected, with the reduction of the S/D. On the contrary, the carrier scattered configuration shows an opposite behaviour. This phenomenon is explained by the fact that the scattering produces near constant signal peak power values, while the signal mean power depend directly on the S/D ratio.

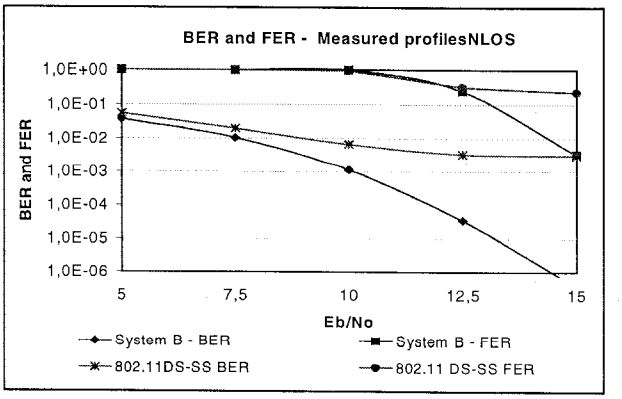

Fig. 8 BER and FER performance of the proposed system in linear NLOS conditions compared with the performance of IEEE 802.11 DS-SS physical layer. In the MCM case dots are relative to simulated performance.

Figure 8 shows the BER performance in NLOS conditions compared with the performance of IEEE 802.11 DS-SS physical layer. The frame length is half the maximum frame length, while the S/D ratio is equal to -3dB for the MCM configuration. The MCM system shows a good matching of the simulation results (dots) with the analytical ones (solid lines). The IEEE 802.11 DS-SS, with DQPSK modulation, shows a worse performance with respect to the proposed MCM system. In the proposed NLOS scenario, indeed, the quality of the channel equalisation is significant and as a consequence the performance margin of the proposed MCM schemes is evident.

A second set of simulations has been carried out in order to evaluate the performance degradation of the proposed MCM system when non linear amplification is considered, both with and without predistortion. The amplifier has been modelled by the distortion curves of Fig.2. The BER performance of the system, with the non linear amplifier only, is shown in Fig.9 for different values of the IBO. The Output Back Off (OBO) corresponding to each value of the IBO is also shown . The system performance of the predistorted amplifier, compared with the ideal situation of interpolated clipping, is also shown in Fig. 10. When IBO value is 9 dB, the clipping phenomenon never occurs because the dynamic range of the signal (i.e. mean crest factor) is lower than the allowed dynamic range of the power amplifier; in this case it is possible to outline the potentiality of the predistortion scheme. Fig. 12 shows, indeed, that the predistorter action is almost perfect since the two BER curves for ideal clipping and predistorted amplifier are practically superimposed; then, in the following, we may consider as a reference for the predistorter performance, those achievable by means of interpolated clipping.

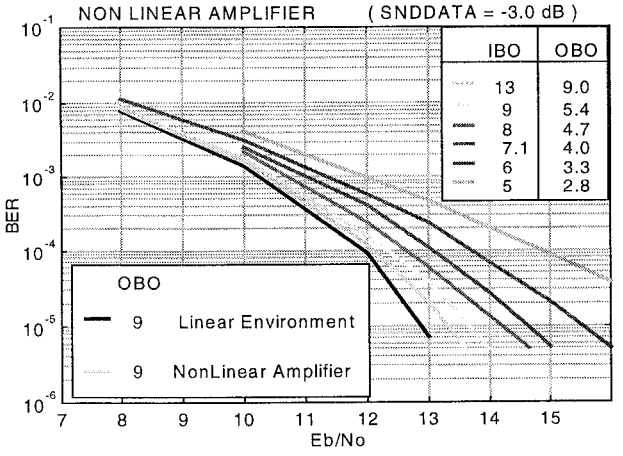

Fig. 9 System Performance with Non Linear Amplifier

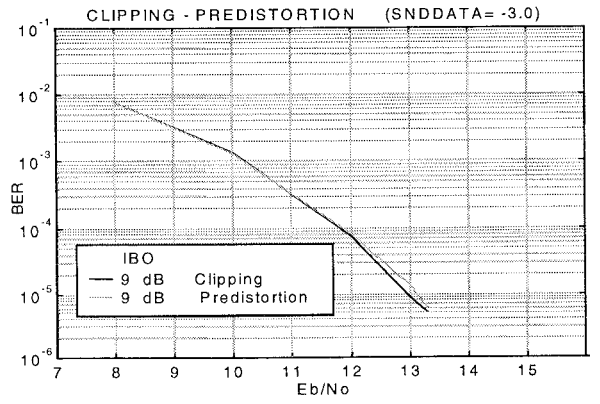

Fig. 10 Performance of predistorted amplifier versus ideal interpolated clipping

We have chosen a BER value of to $1x10^{-5}$ in order to make a comparison of the performance of different system configurations. The key parameters for performance evaluation are described below.

Output Back Off (OBO): when a limit on the maximum signal power is imposed by a saturating amplifier, it is desirable to have the maximum power at the receiver and thus the minimum OBO. (Eb/No): it is proportional to the signal to noise ratio for the data at the receiver side. It is desirable to have the minimum value of Eb/No to accomplish with the required BER value of $1x10^{-5}$. For a fixed modulation scheme this requirement is in conflict with the requirement of a low OBO. A low OBO value, indeed, causes a frequent clipping of the signal. As a consequence higher data power is needed to compensate for the clipping noise in addition to the thermal one.

S/D : the sounding to data power ratio affects the data power efficiency of the system. The total power at the receiver is the sum of sounding power and data power. When the OBO is fixed, the lower the S/D ratio is, the higher data power is. We could define $(OBO)_{eff}$ the effective OBO for the data signal

$$(OBO)_{eff} = \frac{P_{Max}}{P_{DATA}} = \frac{P_{Max}}{P_{TOT}} \cdot \frac{P_{TOT}}{P_{DATA}} = \frac{P_{Max}}{P_{TOT}} \cdot \frac{P_{DATA}+P_{SND}}{P_{DATA}} = OBO \cdot (1+S/D) \quad (26)$$

For S/D values of -6.0,-3.0,and 0 dB the consequent penalty in terms of $(OBO)_{eff}$ is 0.97, 1.76 and 3.0 dB respectively. These penalty values must be added to the OBO values shown in the figure in order to make a comparison with MCM techniques in which the sounding signal is not embedded in the data block as proposed in [6].

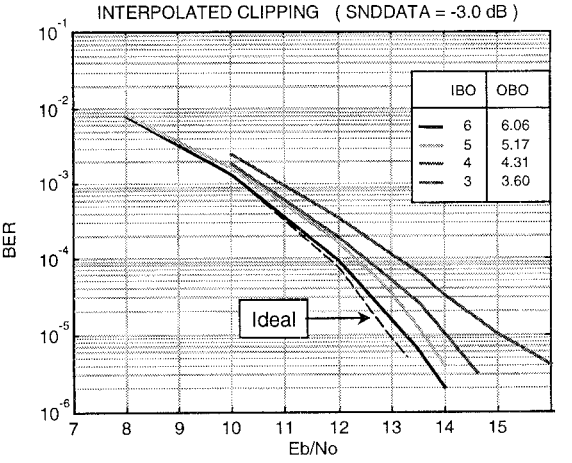

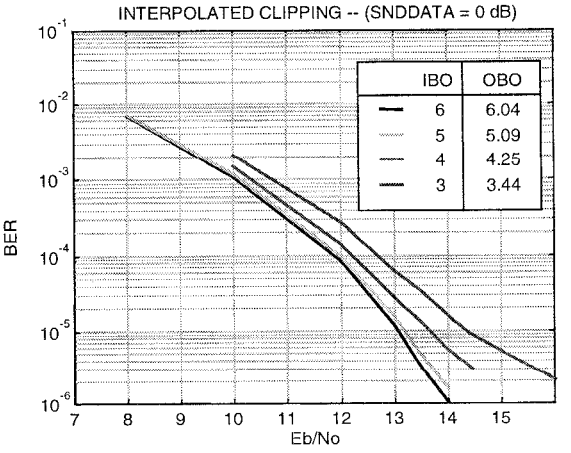

Fig. 11 Performance of Interpolated Clipping for different values of S/D

Looking at Figures 9 and 11 it is possible to compare the performance

of the system with and without predistortion for an S/D value of -3.0 dB. It arises that no great benefits in terms of E_b/N_0 needed to achieve a BER of $1x10^{-5}$ are obtained by the adoption of the predistortion device. In order to obtain the optimum OBO value for the system performance we define the terms Power Gain (PG) as

$$PG(OBO) = [CF - OBO] - \left[(Eb/No)_{OBO} - (Eb/No)_{lin}\right] \quad (27)$$

where $(Eb/No)_{OBO}$ and $(Eb/No)_{lin}$ are the data signal to noise ratio needed to reach a BER of $1x10^{-5}$ for the considered OBO and for the Linear Environment respectively. The situation with an OBO equal to the signal Crest Factor CF, may be considered as linear. By the previous considerations the terms in the first brackets in (27) represent a power gain that grows as the OBO decreases. The second term in (27), on the contrary represents a power penalty, which also increases as OBO decreases. The optimum OBO value is clearly the one that minimises relation (27). The shape of the PG curve is shown in Fig 12 both for interpolated clipping and non linear amplifier with S/D = -3.0 dB. The maximum value for the PG functions is reached for an optimum OBO value of about 4 dB (which corresponds to an $(OBO)_{eff}$ of about 5.7 dB) both for predistorted and not-predistorted situation.

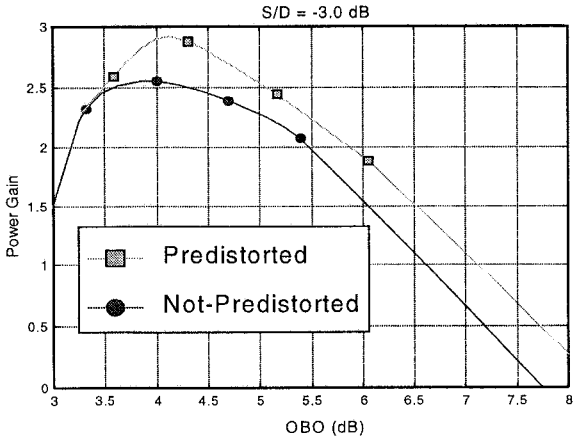

Fig. 12 Power Gain with and without Predistortion

The Power Gain at the receiver is of about 0.4 dB as shown in Figure 12. Greater benefits could be obtained for OBO values comparable with the signal crest factor, using a class B or class C amplifier. Considering Figure 11 it is possible to conclude that an S/D=0 dB must be avoided. Indeed, the gain in terms of E_b/N_0 with respect to S/D=-3.0 dB is too small in comparison to the corresponding $(OBO)_{eff}$ penalty of 1.24 dB (i.e. 3.0 - 1.76 = 1.24). Probably a better compromise could be reached for S/D between -6.0 dB and -3.0 dB.

Conclusions

In this paper a novel radio subsystem for WLAN, based on MCM-DS-SS, has been presented. The proposed MCM-DS-SS architecture has been designed by taking account of the special issues of WLAN applications. In particular, in order to guarantee good throughput values for short packets and for MAC message handshake, a great care has been observed in the strategy adopted for the channel estimation and equalisation, by selecting a simple to implement technique, which avoids the transmission of dedicated sounding symbols. By comparing the achieved performance with the results of the DS-SS physical layer of the IEEE 802.11 standard, we have pointed out some important aspects that might limit the system operation. In particular, the performance of a base-band pre-distorted non-linear amplifier was analysed by simulations. The analysis of the clipping in the non-linear environment allows us to determine the optimum back-off value in order to balance the bit error rate performance and the efficiency of power amplifiers. Taking account of the good capacity for counteracting multipath fading, non linear channels and the obtained value of spectral efficiency we can conclude that the proposed system architecture, combined with baseband predistortion, is an interesting solution for WLAN applications.

References

[1] IEEE 802.11/D2, "Wireless LAN Medium Access Control (MAC) and Physical Layer (PHY) Specifications", Draft Standard, July 1995.

[2] B. Bourin, "HIPERLAN - Markets and Applications Standardisations Issues", IEEE Int. Conf. on Personal, Indoor and Mobile Radio Comm. (PIMRC'94), Hague, Netherlands, pp 863-868, Sept. 1994.

[3] N. Yee, J.P. M.G. Linnartz, G. Fettweis, "Multi-Carrier CDMA in Indoor Wireless Radio Networks", IEICE Trans. on Comm., vol. E77-B, July 1994.

[4] M. Schnell, S. Kaiser, "Diversity Consideration for MC-CDMA systems in Mobile Communications" IEEE International Symposium on Spread Spectrum Techniques and Applications (ISSSTA'96) - Mainz, Germany, September 1996.

[5] R. O'Neill, L.B Lopes, "Performance of Amplitude Limited Multitone Signals", in IEEE VTC'94, June 1994, Stockholm 1994, pp. 1675-1679.

[6] S. Cacopardi, P. Banelli, F. Frescura, G. Reali, "OM-DS-SS Wireless LAN Radio Subsystem: Performance In Clipping Environment Using Measured Channel Delay Profiles", IEEE GLOBECOM '96, London, November 1996, pp. 1897-1903

[7] DVB, "Framing Structure, Channel Coding and Modulation for Digital Terrestrial Television", DVB Document A012, June 1996.

[8] R. L. Frank, S. A. Zadoff, "Phase Shift Pulse Codes with Good Periodic Correlation Properties", IRE Transactions on Information Theory (correspondence), Vol. IT-8, pp. 381-382, Oct. 1962.

[9] M. R. Schroeder, "Synthesis of Low Peak Factor Signals and Binary Sequences with Low Autocorrelation", IEEE Transactions on Information Theory (correspondence), pp. 85-89, January 1970.

[10] D. R. Gimlin, C. R. Patisaul, "On Minimizing the Peak to Average Power Ratio for the Sum of N Sinusoids", IEEE Transactions on Communications, Vol. 41 N°4, pp. 631-635, April 1993.

[11] A.R. Kaye, D.A. George, and M.J. Eric, "Analysis and Compensation of Bandpass Nonlinearity for Communications", IEEE Transactions on Communications, pp. 965-672, October 1972.

[12] S. Cacopardi, F. Frescura, G. Reali, "Performance Comparison of Multicarrier DS-SS Radio Access Schemes for WLAN Using Measured Channel Delay Profiles", IEEE VTC '97, Phoenix, May 1997, pp. 1877-1881

[13] G.Karam and H.Sari, "Generalised Data Predistortion Using Intersymbol Interpolation", Philips Res. Journal, Vol.46, 1991, pp.1-22.

[14] M. Faulkner, M. Yohansson, "Adaptive Linearization Using Predistortion: Experimental Results", IEEE Trans. on Veh. Tech., Vol. VT-43 n.2, May. 1994, pp. 323-332.

[15] H. E. Rowe, "Memoryless Non-Linearities with Gaussian Inputs: Elementary Results", Bell System Technical Journal, Vol. 61 - N° 7, September 1982, pp. 1520-1523.